PLOS ONE

RESEARCH ARTICLE

Novel co-culture plate enables growth dynamic-based assessment of contact-independent microbial interactions

Thomas J. Moutinho, Jr., John C. Panagides, Matthew B. Biggs, Gregory L. Medlock, Glynis L. Kolling, Jason A. Papin*

Department of Biomedical Engineering, University of Virginia, Charlottesville, Virginia, United States of America

* papin@virginia.edu

Citation: Moutinho TJ, Jr., Panagides JC, Biggs MB, Medlock GL, Kolling GL, Papin JA (2017) Novel co-culture plate enables growth dynamic-based assessment of contact-independent microbial interactions. PLoS ONE 12(8): e0182163. https://doi.org/10.1371/journal.pone.0182163

Editor: Jacob Guy Bundy, Imperial College London, UNITED KINGDOM

Received: May 22, 2017

Accepted: July 13, 2017

Published: August 2, 2017

Data Availability Statement: All additional data, code, and CAD files are available at: https://github.com/csbl/CoculturePlate.

Funding: TJM, JCP, MBB, GLM, GLK, and JAP are supported by R01 grant GM108501 from the National Institutes of Health (www.nih.gov). GLM is also supported by National Institute of Health on grant T32LM012416. TJM is also supported by National Science Foundation Graduate Research Fellowship Program DDGE-1315231 (www.nsfgrfp.org). The funders had no role in study

Abstract

Interactions between microbes are central to the dynamics of microbial communities. Understanding these interactions is essential for the characterization of communities, yet challenging to accomplish in practice. There are limited available tools for characterizing diffusion-mediated, contact-independent microbial interactions. A practical and widely implemented technique in such characterization involves the simultaneous co-culture of distinct bacterial species and subsequent analysis of relative abundance in the total population. However, distinguishing between species can be logistically challenging. In this paper, we present a low-cost, vertical membrane, co-culture plate to quantify contact-independent interactions between distinct bacterial populations in co-culture via real-time optical density measurements. These measurements can be used to facilitate the analysis of the interaction between microbes that are physically separated by a semipermeable membrane yet able to exchange diffusible molecules. We show that diffusion across the membrane occurs at a sufficient rate to enable effective interaction between physically separate cultures. Two bacterial species commonly found in the cystic fibrotic lung, *Pseudomonas aeruginosa* and *Burkholderia cenocepacia*, were co-cultured to demonstrate how this plate may be implemented to study microbial interactions. We have demonstrated that this novel co-culture device is able to reliably generate real-time measurements of optical density data that can be used to characterize interactions between microbial species.

Introduction

There exists an extensive amount of interaction among microorganisms in microbial communities [1–3]. An improved understanding of these interactions and their governing mechanisms in a physiologically relevant context will enable more informed treatment of polymicrobial infections and more precise modulation of microbial communities [4–6]. Interactions between microbes are characterized using a variety of methods [7]. Many interactions that take place within microbial communities are due to diffusible molecules such as cross-fed

design, data collection and analysis, decision to publish, or preparation of the manuscript.

Competing interests: The authors have declared that no competing interests exist.

metabolites, quorum sensing molecules, and antimicrobial compounds [8,9]. Interactions mediated via diffusible molecules generally do not require the physical interaction of cells and are thus contact-independent [10–13]. These interactions are challenging to characterize with existing approaches [11].

Common co-culture techniques include well mixed co-cultures [14], conditioned media exchange [15], agar plate colony assays [16,17], and membrane divided co-culture such as Corning® Transwell® co-culture plates [18]. Each of these methods are limited in their ability to phenotypically characterize the growth dynamics of the microbes in co-culture. In a mixed co-culture it is challenging to measure the individual growth curves of the two species using high-throughput techniques. It is possible to use qPCR techniques to determine the relative abundance of each species; however, this is a technically and logistically challenging experimental technique requiring the development of specific primers for each species [19,20]. Conditioned media exchange experiments are limited to unidirectional interactions which do not capture the dynamic response of cells to changing conditions [15]. Corning® Transwell® culture plates keep cells physically separate while allowing for contact-independent interactions, yet the horizontal membrane does not allow for the collection of optical density based continuous growth curve data for each culture.

Since the advent of semipermeable membrane-divided co-culture tools [21,22], to the best of our knowledge, this concept has never been interfaced with automated plate reader technology for the high-throughput continuous quantification of optical density-based phenotypic assessment of interacting cultures. Optical density of liquid bacterial cultures has been used for a multitude of phenotypic studies that aim to determine the relative changes in cellular growth subject to various environmental conditions [23–28]. We present a novel co-culture plate with a vertically oriented membrane that maintains physical separation of two liquid cultures, yet allows for real-time contact-independent interactions across the membrane. The vertically oriented membrane allows for the co-culture plate to interface with a standard 96-well plate reader that is able to continuously monitor the optical density of both cultures on either side of the membrane. This culture tool is a simple, convenient, and inexpensive method for generating individual growth curves of two batch bacterial cultures as they interact across a membrane.

Materials and methods

Strain information

We used *Escherichia coli* (K12), *Pseudomonas aeruginosa* (PA14), and *Burkholderia cenocepacia* (K56-2) in this study.

Media preparation

Lysogeny broth–Miller (LB) medium: tryptone (10g/L), yeast extract (5g/L), NaCl (10g/L), pH was adjusted to 7.0 with NaOH. In several experiments the LB media was diluted with 1x Dulbecco's Phosphate Buffered Saline (DPBS) (Gibco by Life Technologies). This dilution is indicated throughout the paper as the percentage of LB that is in the diluted media.

Sterilization procedures

Before each experiment all parts of the co-culture plate were steam autoclaved at 121˚C, 100kPa, for 60 minutes. The polycarbonate membranes (Isopore™ Membrane Filter, 0.1 μm VCTP; EDM Millipore) were prepared by soaking in 70% ethanol for 10 minutes. For further description and rationale, see S1 Appendix. In a biosafety cabinet, the ethanol-soaked

membranes were clamped between the wells and the assembly was left for 10 minutes to allow the ethanol to evaporate. For plate assembly protocol and visual aids, see S1 Appendix.

Counting of Colony Forming Units (CFUs)

CFUs were counted as previously reported [29]. Briefly, a serial dilution down to 10^{-7} for each of the original cultures was prepared, 10 μL of each dilution was dripped onto LB agar plates and left to dry for roughly 10 minutes. The CFU plates were then incubated for the appropriate amount of time for visible colony growth. Colonies were then manually counted. Reported counts were done in quadruplicate (n = 4).

Growth curve collection and processing

Each well of the co-culture plate was loaded with 2 mL of media. Where appropriate, wells were inoculated at a calculated OD_{600} of 0.0005 with the bacterial strain specified. The co-culture plate was then placed into a Tecan Infinite M200 Pro plate reader, incubated at 37˚C, shaken linearly with 3 mm of travel at 7.5 hertz (450 RPM), and OD measurements were recorded at 600 nm every 5 minutes. All of the experiments were conducted in triplicate with biological replicates. The data from each experiment was exported as an Excel file and processed in MATLAB (R2014b; Mathworks). In all figures, the growth curve plots consist of the average (bold line) displayed with the maximum and minimum values (as shaded regions around the average line). All growth experiments were conducted in triplicate. The MATLAB scripts used for all data processing are available, refer to the Availability section.

Scanning Electron Microscopy (SEM)

Following an *E. coli* experiment with the co-culture plate, the polycarbonate membranes were fixed for 30 minutes with glutaraldehyde (2% by vol.). Followed by three 5-minute rinse steps in 1x DPBS. Samples were then dehydrated using increasing concentrations of ethanol, 10 minutes each in 30, 50, 70, 80, 90, 100, 100% (ethanol in water). The membranes were further dehydrated for 10 minutes in HMDS (hexamethyldisilazane; Sigma). Finally, the membranes were stuck to SEM stubs with adhesive carbon strips using the Phenom starter kit (Ted Pella, Redding, CA, USA) and sputter coated with gold using a SCD005 sputter coater (Bal-tec, Los Angeles, CA, USA). The final samples were imaged using a Sigma VP HD Field-emission SEM (Zeiss, Pleasanton, CA, USA) at 10,000x magnification through the University of Virginia Advanced Microscopy Facility.

Device design and machining

All of the parts for the co-culture plate were designed in SolidWorks 2015; all of these files are available, refer to the Availability section. The files were exported as STL files (also available) and G-code was written for CNC machining. The aluminum parts were cut using a waterjet cutter and the holes were tapped by hand. The polypropylene wells were started using a waterjet cutter and finished using a milling machine. The polycarbonate was also cut using the waterjet cutter. All parts are designed to be able to be CNC machined without the use of a waterjet cutter. The silicone gaskets were made using a laser cutter (Universal laser Systems X-660 with a 50 watt CO_2 laser). For a detailed list of the parts please refer to the S1 Appendix and for the manufactured part specifications see S1 Technical Drawings.

Results

Design and description

The vertical membrane co-culture plate consists of eight co-culture chambers, each chamber is composed of two wells separated by a membrane that is replaced before each experiment. Each well is designed to hold 2 mL of culture and thus 4 mL of total liquid in each chamber. All of the materials used for the body of the plate can be sterilized via autoclave. The outer dimensions and wells on the plate line up with the dimensions and wells of a standard Corning® 96-well plate, allowing it to interface with any plate reader designed to read 96-well plates. Each of the co-culture wells lines up with two wells on a 96-well plate, allowing for an internal technical replicate to be collected for each well to reduce noise (Fig 1A).

The well walls are machined polypropylene, bolted to a machined aluminum base. Clamped between the polypropylene wells and aluminum base are clear polycarbonate pieces acting as the bottom of the wells. A silicone gasket creates a liquid tight seal on the bottom edge of the

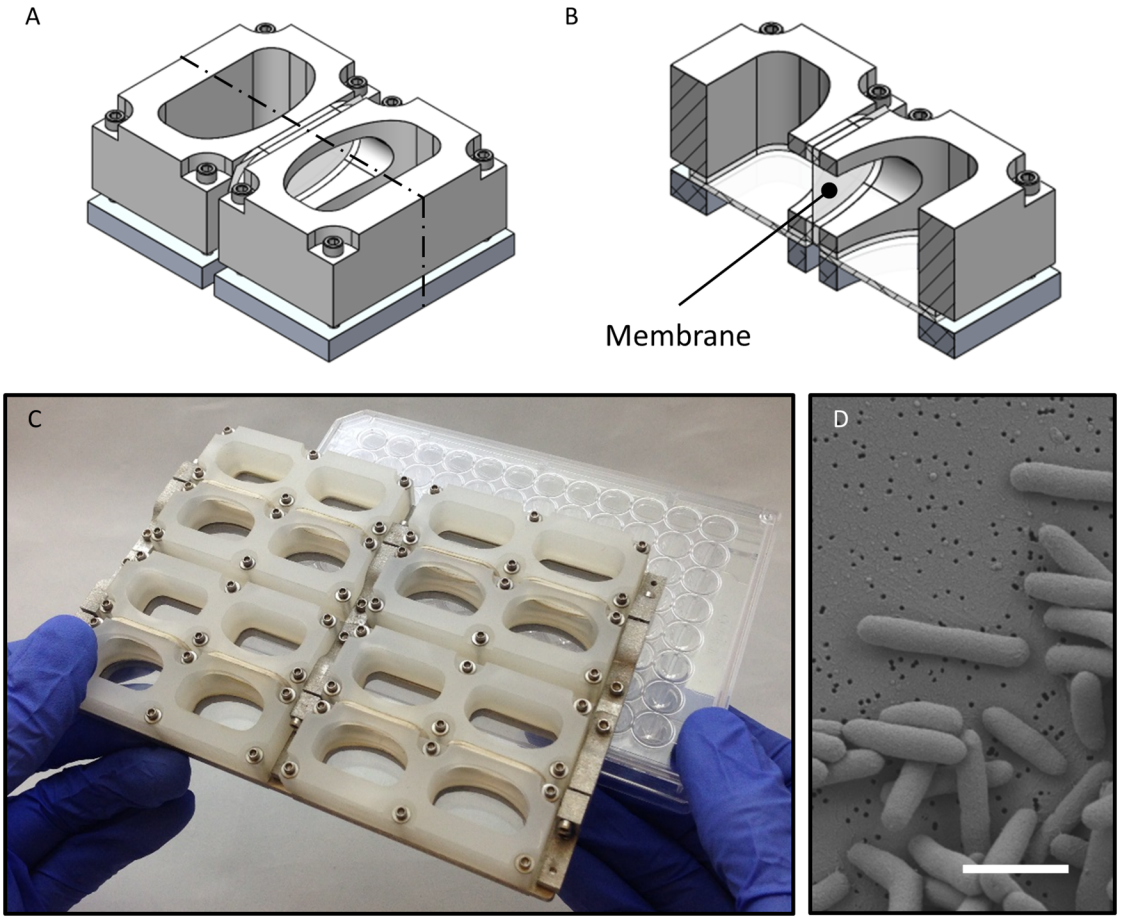

Fig 1. Co-culture plate design. The co-culture plate consists of eight individual co-culture chambers. Each chamber consists of two wells that are able to hold liquid cultures that are physically separated by a semi-permeable membrane that allows for diffusion-mediated interactions. A representative isometric mechanical drawing of a single co-culture chamber is shown in (A), note it is composed of two wells. For a better view of the wells, a cross-sectional view is shown in (B); the semi-permeable membrane is labelled. The co-culture plate, composed of eight co-culture chambers, has the same profile as a standard 96-well plate. Each well on the co-culture plate aligns with two wells of a 96-well plate and the culture volume is 2 mL per well (4 mL total per chamber) (C). An SEM image captures *E. coli* cells fixed on the surface of a polycarbonate membrane with 0.1 μm pores (D); the scale bar is 2 μm.

https://doi.org/10.1371/journal.pone.0182163.g001

wells. Additional silicone gaskets are adhered to the side ports in the well walls to create a seal against the membrane which is clamped between the wells. The location of the membrane is indicated in Fig 1B. Any type of membrane can be used in this plate.

The base of the plate is composed of three separate parts. Each of the wells is first clamped onto the three base parts and these parts are subsequently clamped together horizontally after the membranes are in place. The dual clamping design allows for adequate force to be applied to create water tight seals both against the bottom of the wells and the sides where the membranes are placed. For further description of the design and machining of the plate, as well as a video of the assembly, refer to the S1 Appendix.

Validation

The co-culture plate was evaluated for basic functions to guide the interpretation of the data generated using this novel platform. First, we explored whether the rate of metabolite diffusion across the membrane would influence growth dynamics of a culture. Second, we confirmed that the membrane was a sufficient barrier to maintain physical isolation between wells. Finally, we characterized interactions of a microbe with itself across the membrane, as a control for later multi-species co-cultures.

We characterized the impact that diffusion of metabolites across the membrane might have on growth characteristics. We measure the growth of *E. coli* in two conditions, 'pre-mixed' and 'gradient', at four concentrations of LB (Fig 2). The 'pre-mixed' condition is inoculated on one side of the membrane and has equal concentrations of LB (diluted with DPBS) on either side. The 'gradient' condition is also inoculated on one side of the membrane, but starts with all of the LB on the opposite side. Therefore, for growth to occur on the DPBS-inoculated side, the LB must diffuse across the membrane. The total quantity of LB provided between each

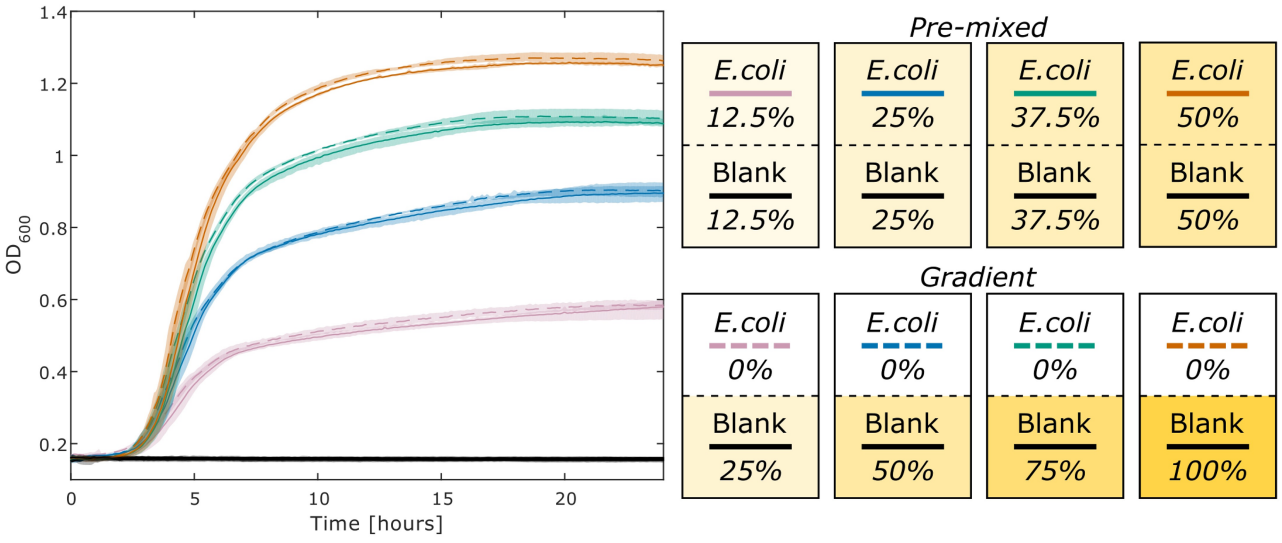

Fig 2. Real-time diffusion of metabolites across a membrane. One side of each co-culture chamber was inoculated with *E. coli*, as seen in the pictorial legend on the right, each box represents a chamber with a black dashed line representing the membrane. The terms 'pre-mixed' and 'gradient' describe the initial media conditions. The gradient condition was loaded with LB on one side and 1x DPBS on the other. The pre-mixed condition was loaded with LB that was diluted in half with DPBS to simulate complete diffusion of LB across the membrane. These two conditions were tested with four initial concentrations of LB, 25%, 50%, 75%, and 100%, all diluted using 1x DPBS. The final pre-mixed concentration of the medium for each well was 12.5%, 25%, 37.5%, and 50% LB. The maximum and minimum values of the generated growth curves, conducted in triplicate (n = 3), are displayed as shaded regions around the plotted averages. This experiment was cultured as described in the methods for 24 hours.

https://doi.org/10.1371/journal.pone.0182163.g002

condition was held constant. These two conditions were assayed at four different concentrations to demonstrate the observed behavior at various concentration gradients across the membrane, ranges of maximum optical density, and resulting population densities. We observe that there are only slight differences between the paired conditions at all four concentrations. These results indicate that the essential metabolites in LB are able to diffuse across the membrane at a sufficiently rapid rate to allow *E. coli* to grow similarly to the control case.

The data for Fig 2 was generated in triplicate such that there were 24 individual co-culture chambers inoculated on one side of the membrane only. Of these 24 individual cases, the optical density of the negative control side was measured to test that the membrane serves as a sufficient barrier to *E. coli* crossing from one well to the other. We never observed *E. coli* contamination from one well to the other, therefore the design of the plate and size of the pores in the membrane (Fig 1D) are sufficient to maintain complete physical separation between the two wells of each chamber and yet allow for the exchange of nutrients and small molecules to support growth without a notable defect in the associated growth dynamics for the conditions we tested. Pictures of the plate can be seen with co-cultures at the end point in S1 Fig.

One potential application for this co-culture plate is the characterization of growth dynamics for two different species on either side of the membrane. To determine the basic characteristics of co-culture between competing cultures, we cultured *E. coli* in isolation on one side of a chamber and two *E. coli* populations separated by the membrane, thus competing for nutrients, in another chamber (Fig 3). Both of these conditions were assessed at 50% LB (diluted with 1x DPBS) and 100% LB. The condition in which *E. coli* is isolated on just one side of the co-culture chamber acts as a reference point compared to the case in which two *E. coli*

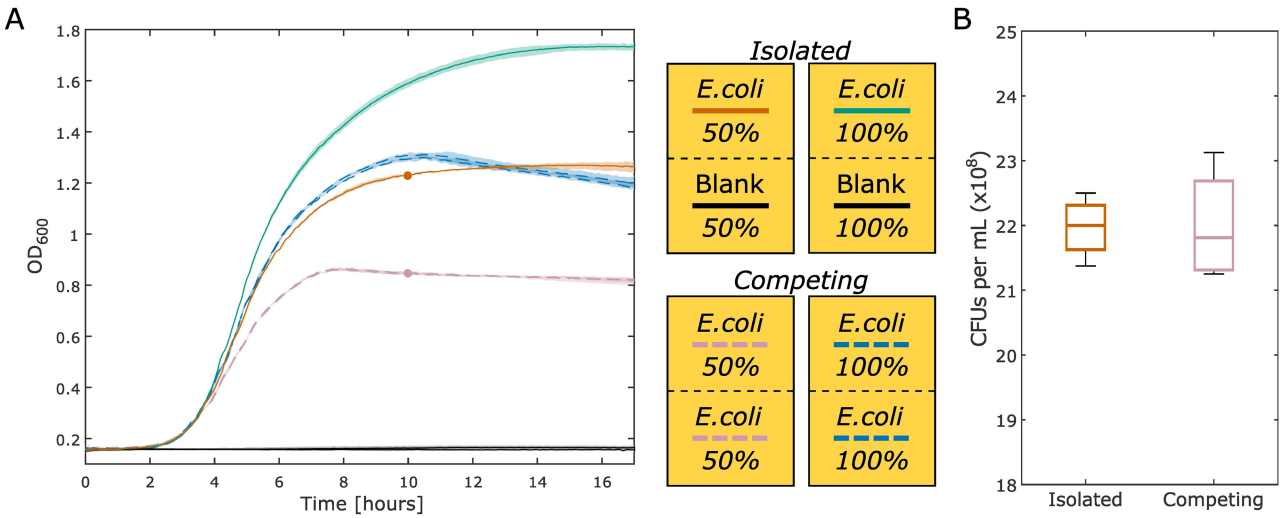

Fig 3. Comparison of isolated versus competing cultures. (A) The green (100% LB) and orange (50% LB) lines are the isolated culture condition that have *E. coli* cultured on only one side of the membrane with blank media on the other. The OD for the side of the well that is not inoculated is plotted in black (it maintains the original OD; there is no growth, as expected). In this condition, *E. coli* has access to all of the nutrients on both sides of the membrane, but cell growth is physically constrained to one side. The blue (100% LB) and purple (50% LB) dashed lines are the competing culture condition that have *E. coli* cultured on both sides of the membrane. For the competing cultures, the growth curves from both sides are plotted individually. In this condition, each *E. coli* population must compete for the available nutrients. The maximum and minimum values of the generated growth curves, conducted in triplicate, are displayed as shaded regions around the plotted averages. (B) The biomass produced from the 50% LB isolated (solid orange) and competing (dashed purple) conditions at 10 hours is approximated by the CFU count of each culture. The CFU counts for the isolated condition as displayed are divided in half to compare to the competing condition, discussed further in the text. These data are the result of four experiments. The boxplot whiskers represent +/- 2.7σ from the mean.

https://doi.org/10.1371/journal.pone.0182163.g003

populations are competing. For the condition in which *E. coli* is competing and cultured with 100% LB, the growth characteristics are similar to those observed when *E. coli* is isolated and cultured in 50% LB. This indicates that there is a comparable amount of biomass produced on either side of the membrane in the 100% LB competing case to the amount of biomass produced in the 50% LB isolated case. The slight differences between these curves represent a situation in which there are fascinating growth dynamics across the membrane that can be further explored utilizing this co-culture plate.

A follow up experiment was conducted to determine if the same number of CFUs, from both sides of the membrane, are produced in the competing versus the isolated conditions. Samples were taken from the 50% LB isolated (solid red) and competing (dashed purple) conditions at 10 hours into incubation. The 50% LB condition was chosen to limit the impact of OD non-linearity and inhibition of growth due to spatial restrictions, therefore prioritizing nutrient depletion as the major limiting factor of biomass production. The bacteria were diluted, plated, and CFUs were counted (Fig 3B). The CFU counts for the isolated condition were divided in half to adequately compare to one side of the competing condition. This was done because all of the biomass in the isolated case is located on one side whereas the biomass is split evenly on either side in the competing condition. It can be seen that the same total number of CFUs are present in both the competing and the isolated conditions from Fig 3A. The equivalence between the two conditions in this boxplot indicates that the same number of viable cells are produced in the two different conditions. These data indicate that the competing condition for a certain microbe and media condition can act as an approximation for the hypothetical case in which two different species in co-culture on either side are in complete metabolic competition with each other. In this context, complete metabolic competition means that the cultures on either side have the same metabolic requirements, this is only the case when the same species are on both sides of the membrane. The growth curve representing complete metabolic competition can be used in tandem with the isolated condition in which there is no metabolic competition for a phenotypic assessment of interactions between two different species in co-culture across the membrane.

Co-culture of multiple species

Infection with *P. aeruginosa* (PA) is pervasive in cystic fibrosis patients [30]. Co-infection with *B. cenocepacia* (BC) can lead to increased mortality rates [31]. These pathogens have been shown to interact in cystic fibrosis infections [32]. We used the co-culture plate to determine the growth characteristics when PA and BC in which media, nutrients, and small molecules are shared. The condition where a microbe is competing with itself across the membrane is an approximation of complete metabolic competition. The competing and isolated conditions, as defined in Fig 3, can be used as points of reference when assessing the impact another species has on a culture. In this case, we observe that when PA and BC are co-cultured, BC growth is negatively impacted by the presence of PA (dashed purple), more so than when it is competing with itself (dashed orange). However, it appears that PA is unaffected by the presence of BC (solid purple vs. solid blue). This interaction between PA and BC has been observed previously in liquid LB, BC growth is shown via qPCR to be severely reduced at a single time point when in a mixed co-cultured with PA [33]. This interaction appears to be, in part, a function of pyoverdine production as indicated in two *in vitro* studies [33,34].

Discussion

In this study, we present a novel tool to enable dynamic growth measurements of individual species interacting in co-culture. Mixed co-culture studies rely on a number of methods for

differentiating between specific species when a semi-permeable barrier is not utilized. CFU assays for mixed co-cultures require that populations can be discriminated based on colony morphology, and flow cytometry based counting assays require discrimination by cellular morphology or fluorescence staining [35,36]. However, these assays cannot be used to study co-cultures of morphologically similar populations. Species-specific qPCR assays can be used when genomic sequences are available; fluorescent primers are used to discriminate between microbial DNA [19,35,37,38]. However, manual sampling requires sufficient volume for DNA extraction and therefore greatly constrains possible experimental designs. This requirement of large culture volumes is a limitation shared by all methods that require periodic manual or automated sampling of the culture. Additionally, qPCR assays must be developed for each species in a co-culture study while limiting nonspecific amplification and ensuring stability of the primers [35]. While most of these methods can be used in a broader context than batch co-culture in a liquid medium, the experimental design and optimization required for them limits throughput relative to the co-culture plate presented here.

As presented, this novel co-culture plate is able to maintain physical separation of two interacting cultures, while allowing for diffusion mediated interactions. Metabolites across the membrane appear to diffuse across at a sufficiently high rate to not be a limiting factor for growth dynamics. We are able to use the plate to investigate the co-culture of two different species with the use of self-competing controls and isolated culture controls. These controls can be used as a reference for the experimental condition of two species interacting across the membrane.

A particular strength of this co-culture plate is the ability to measure optical density data in real-time. This high temporal resolution captures complex growth dynamics that might not be observed with methods that require manual sampling of the culture. Separating the microbial cultures with a membrane eliminates the need to differentiate the individual species in co-culture. Furthermore, no genetic tools are required in order to screen microbes in this co-culture plate. One possible use of this device could be to co-culture a single species in one well with a complex community in the other well. Although it is not developed here, the wells on the co-culture plate have an adequate volume of media to allow for additional 'omics' based analyses (i.e. transcriptomics, proteomics, metabolomics, and metagenomics) to be conducted on the cultures at the end point of the experiment. Furthermore, this novel tool makes it exceptionally simple to generate phenotypic data on the dynamic interactions between two microbial species. The setup for such an experiment (e.g. Fig 4) requires less than two hours.

Although the proposed co-culture plate, in its current form, accommodates only one complete two species interaction experiment, throughput can be improved in two ways. Parallelized experiments using additional co-culture plates in conjunction with miniaturized plate readers [39] allows for the collection of endpoint metabolomics samples. As for experiments that do not require such culture volumes, the current co-culture plate design could be scaled down to a format with a greater number of smaller wells. This redesign would be optimized for rapid assays to identify biologically interesting pairs. Additional limitations of the proposed co-culture plate include the restriction to batch culture experiments, the lack of being able to assess contact-dependent interactions due to physical separation with the membrane, and the biofouling of the membrane. Membrane biofouling is a well-recognized issue when utilizing membranes in biological reactors [40]. Although it is primarily an issue in systems that have a pressure differential across the membrane, there remains concern that the diffusivity of the membranes in the co-culture plate gradually decreases over time as cells adhere to it. However, the choice of a polycarbonate membrane in this study was made due to its low protein adsorption properties.

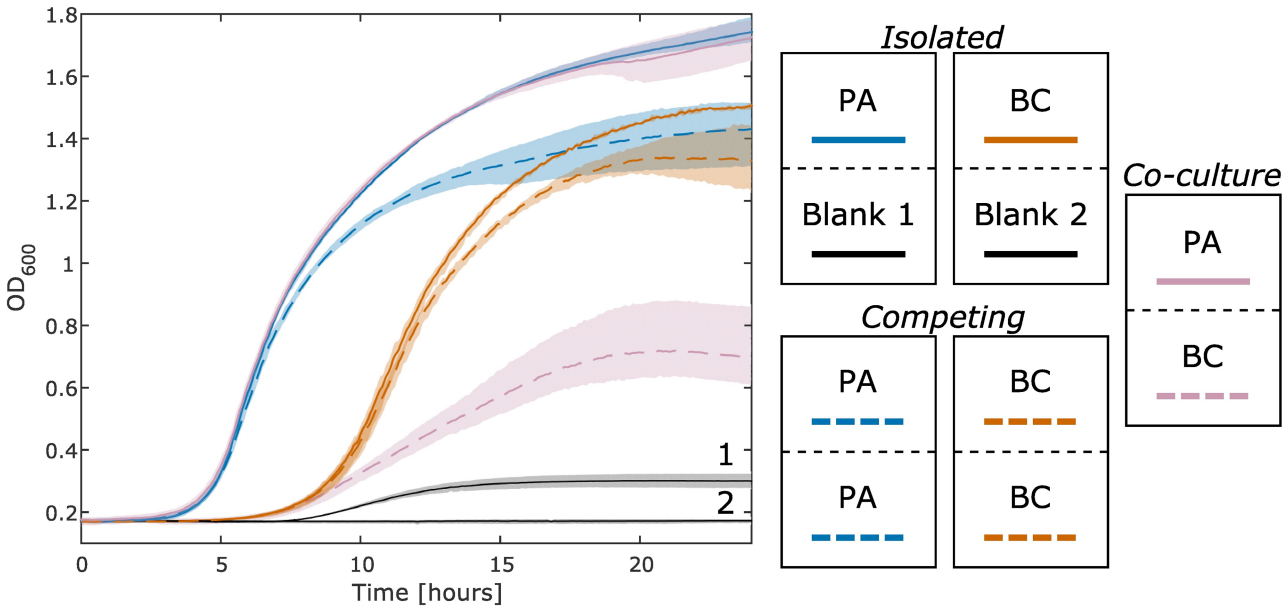

Fig 4. Growth curves of *P. aeruginosa* (PA) and *B. cenocepacia* (BC) in co-culture. The culture conditions can be seen in the legend on the right side of this figure. All wells are started with 100% LB. The purple lines are gathered from the co-culture of PA and BC. The isolated PA and BC cultures are the solid blue and orange lines respectively. The black lines are controls from the side of the wells that were not inoculated for the isolated PA and BC cultures. The black line slightly increases (Blank 1) as a result of pyoverdine (produced by PA) that partially absorbs at 600 nm. This result is discussed further in the Supporting information (S2 Fig). The growth curves from each of the two competing PA and BC cultures (dashed blue and orange lines respectively) are nearly identical (similar to blue and purple in Fig 3) and thus are averaged to simplify the plot. The maximum and minimum values of the generated growth curves, conducted in triplicate (n = 3), are displayed as shaded regions around the plotted averages.

https://doi.org/10.1371/journal.pone.0182163.g004

In conclusion, we have presented a novel co-culture plate that utilizes a vertical membrane to maintain physical separation between two cultures, yet allows for contact-independent interactions. This culture plate allows for high-throughput and high-resolution phenotypic assessment of microbial interactions. As well as interfacing with currently available plate readers, thus allowing for the rapid generation of optical density growth curves.

Supporting information

S1 Appendix. Additional information about the manufacture and use of the co-culture plate. This document contains a parts list for the plate, a detailed explanation of the design of the plate, and a protocol for using the plate.
(PDF)

S1 Fig. Endpoint image of co-culture plate after representative experiment from Fig 2. Note that the lower wells are all devoid of bacterial growth, while the well on the other side of the membrane is inoculated with an active culture of *E. coli*. Sterility of the wells is maintained by the membranes.
(PDF)

S2 Fig. Co-culture of *P. aeruginosa* and B. Cenocepacia. Well 1a is PA, 1b is BC, 5a and 5b are a technical replicate of that, these are the experimental co-cultures. Wells 3a and 3b are the isolated condition of PA, 7a and 7b are the competing condition. Wells 4a and 4b are the isolated condition of BC, 8a and 8b are the competing condition. Wells 2a, 2b, 6a, and 6b are the isolated and competing conditions for PA and BC mixed, these data are not presented in the

manuscript. *P. aeruginosa* shows clear production of pyoverdine (green pigment) in the chambers it is cultured in. The production of pyoverdine has been previously reported [41].
(PDF)

S1 Technical Drawings. A document containing the technical drawings for each part. Although these drawings have the specifications for machining the parts, it is recommended that each part is machined based on the CAD files using a CNC machine.
(PDF)

Acknowledgments

The authors thank Nick Anselmo for generating the CNC Machine G-code and machining the parts for the co-culture plate.

Author Contributions

Conceptualization: Thomas J. Moutinho, Jr., John C. Panagides, Matthew B. Biggs, Glynis L. Kolling, Jason A. Papin.

Data curation: Thomas J. Moutinho, Jr., John C. Panagides.

Formal analysis: Thomas J. Moutinho, Jr., John C. Panagides.

Funding acquisition: Thomas J. Moutinho, Jr., Matthew B. Biggs, Gregory L. Medlock, Glynis L. Kolling, Jason A. Papin.

Investigation: Thomas J. Moutinho, Jr., John C. Panagides.

Methodology: Thomas J. Moutinho, Jr., Matthew B. Biggs, Glynis L. Kolling, Jason A. Papin.

Project administration: Thomas J. Moutinho, Jr.

Resources: Thomas J. Moutinho, Jr., Glynis L. Kolling, Jason A. Papin.

Software: Thomas J. Moutinho, Jr., John C. Panagides.

Supervision: Thomas J. Moutinho, Jr., Matthew B. Biggs, Glynis L. Kolling, Jason A. Papin.

Validation: Thomas J. Moutinho, Jr.

Visualization: Thomas J. Moutinho, Jr., John C. Panagides, Matthew B. Biggs, Gregory L. Medlock, Glynis L. Kolling, Jason A. Papin.

Writing – original draft: Thomas J. Moutinho, Jr., John C. Panagides, Matthew B. Biggs, Gregory L. Medlock, Glynis L. Kolling, Jason A. Papin.

Writing – review & editing: Thomas J. Moutinho, Jr., John C. Panagides, Matthew B. Biggs, Gregory L. Medlock, Glynis L. Kolling, Jason A. Papin.

References

1. Xavier JB. Social interaction in synthetic and natural microbial communities. Mol Syst Biol. 2011; 7: 483. https://doi.org/10.1038/msb.2011.16 PMID: 21487402
2. Braga RM, Dourado MN, Araújo WL. Microbial interactions: ecology in a molecular perspective. Braz J Microbiol. 2016; 47, Supplement 1: 86–98. https://doi.org/10.1016/j.bjm.2016.10.005 PMID: 27825606
3. Ponomarova O, Patil KR. Metabolic interactions in microbial communities: untangling the Gordian knot. Curr Opin Microbiol. 2015; 27: 37–44. https://doi.org/10.1016/j.mib.2015.06.014 PMID: 26207681
4. Wright C j., Burns L h., Jack A a., Back C r., Dutton L c., Nobbs A h., et al. Microbial interactions in building of communities. Mol Oral Microbiol. 2013; 28: 83–101. https://doi.org/10.1111/omi.12012 PMID: 23253299

5. Ramsey MM, Rumbaugh KP, Whiteley M. Metabolite Cross-Feeding Enhances Virulence in a Model Polymicrobial Infection. PLOS Pathog. 2011; 7: e1002012. https://doi.org/10.1371/journal.ppat.1002012 PMID: 21483753
6. Oliveira NM, Niehus R, Foster KR. Evolutionary limits to cooperation in microbial communities. Proc Natl Acad Sci U S A. 2014; 111: 17941–17946. https://doi.org/10.1073/pnas.1412673111 PMID: 25453102
7. Goers L, Freemont P, Polizzi KM. Co-culture systems and technologies: taking synthetic biology to the next level. J R Soc Interface. 2014; 11: 20140065. https://doi.org/10.1098/rsif.2014.0065 PMID: 24829281
8. Hibbing ME, Fuqua C, Parsek MR, Peterson SB. Bacterial competition: surviving and thriving in the microbial jungle. Nat Rev Microbiol. 2010; 8: 15–25. https://doi.org/10.1038/nrmicro2259 PMID: 19946288
9. Wintermute EH, Silver PA. Dynamics in the mixed microbial concourse. Genes Dev. 2010; 24: 2603–2614. https://doi.org/10.1101/gad.1985210 PMID: 21123647
10. Miller MB, Bassler and B L. Quorum Sensing in Bacteria. Annu Rev Microbiol. 2001; 55: 165–199. https://doi.org/10.1146/annurev.micro.55.1.165 PMID: 11544353
11. Phelan VV, Liu W-T, Pogliano K, Dorrestein PC. Microbial metabolic exchange—the chemotype-to-phenotype link. Nat Chem Biol. 2012; 8: 26–35. https://doi.org/10.1038/nchembio.739 PMID: 22173357
12. Morris BEL, Henneberger R, Huber H, Moissl-Eichinger C. Microbial syntrophy: interaction for the common good. FEMS Microbiol Rev. 2013; 37: 384–406. https://doi.org/10.1111/1574-6976.12019 PMID: 23480449
13. Linares JF, Gustafsson I, Baquero F, Martinez JL. Antibiotics as intermicrobial signaling agents instead of weapons. Proc Natl Acad Sci. 2006; 103: 19484–19489. https://doi.org/10.1073/pnas.0608949103 PMID: 17148599
14. Wintermute EH, Silver PA. Emergent cooperation in microbial metabolism. Mol Syst Biol. 2010; 6: 407. https://doi.org/10.1038/msb.2010.66 PMID: 20823845
15. Biggs MB, Medlock GL, Moutinho TJ, Lees HJ, Swann JR, Kolling GL, et al. Systems-level metabolism of the altered Schaedler flora, a complete gut microbiota. ISME J. 2017; 11: 426–438. https://doi.org/10.1038/ismej.2016.130 PMID: 27824342
16. Traxler MF, Watrous JD, Alexandrov T, Dorrestein PC, Kolter R. Interspecies Interactions Stimulate Diversification of the Streptomyces coelicolor Secreted Metabolome. mBio. 2013; 4: e00459–13. https://doi.org/10.1128/mBio.00459-13 PMID: 23963177
17. Liu A, Archer AM, Biggs MB, Papin JA. Growth-altering microbial interactions are responsive to chemical context. PLOS ONE. 2017; 12: e0164919. https://doi.org/10.1371/journal.pone.0164919 PMID: 28319121
18. Stadie J, Gulitz A, Ehrmann MA, Vogel RF. Metabolic activity and symbiotic interactions of lactic acid bacteria and yeasts isolated from water kefir. Food Microbiol. 2013; 35: 92–98. https://doi.org/10.1016/j.fm.2013.03.009 PMID: 23664259
19. Savichtcheva O, Joris B, Wilmotte A, Calusinska M. Novel FISH and quantitative PCR protocols to monitor artificial consortia composed of different hydrogen-producing Clostridium spp. Int J Hydrog Energy. 2011; 36: 7530–7542. https://doi.org/10.1016/j.ijhydene.2011.03.097
20. Bustin SA, Beaulieu J-F, Huggett J, Jaggi R, Kibenge FS, Olsvik PA, et al. MIQE précis: Practical implementation of minimum standard guidelines for fluorescence-based quantitative real-time PCR experiments. BMC Mol Biol. 2010; 11: 74. https://doi.org/10.1186/1471-2199-11-74 PMID: 20858237
21. Boyden S. The chemotactic effect of mixtures of antibody and antigen on polymorphonuclear leucocytes. J Exp Med. 1962; 115: 453–466. PMID: 13872176
22. Nurmikko V. Microbiological Determination of Vitamins and Amino Acids Produced by Microorganisms, Using the Dialysis Cell. Appl Microbiol. 1957; 5: 160–165. PMID: 13435728
23. Dalgaard P, Ross T, Kamperman L, Neumeyer K, McMeekin TA. Estimation of bacterial growth rates from turbidimetric and viable count data. Int J Food Microbiol. 1994; 23: 391–404. https://doi.org/10.1016/0168-1605(94)90165-1 PMID: 7873339
24. Jung PP, Christian N, Kay DP, Skupin A, Linster CL. Protocols and Programs for High-Throughput Growth and Aging Phenotyping in Yeast. PLOS ONE. 2015; 10: e0119807. https://doi.org/10.1371/journal.pone.0119807 PMID: 25822370
25. Mytilinaios I, Bernigaud I, Belot V, Lambert R j. Microbial growth parameters obtained from the analysis of time to detection data using a novel rearrangement of the Baranyi–Roberts model. J Appl Microbiol. 2015; 118: 161–174. https://doi.org/10.1111/jam.12695 PMID: 25393511

26. Nakagawa A, Minami H, Kim J-S, Koyanagi T, Katayama T, Sato F, et al. A bacterial platform for fermentative production of plant alkaloids. Nat Commun. 2011; 2: 326. https://doi.org/10.1038/ncomms1327 PMID: 21610729

27. Cope EK, Goldstein-Daruech N, Kofonow JM, Christensen L, McDermott B, Monroy F, et al. Regulation of Virulence Gene Expression Resulting from Streptococcus pneumoniae and Nontypeable Haemophilus influenzae Interactions in Chronic Disease. PLOS ONE. 2011; 6: e28523. https://doi.org/10.1371/journal.pone.0028523 PMID: 22162775

28. Zhou K, Qiao K, Edgar S, Stephanopoulos G. Distributing a metabolic pathway among a microbial consortium enhances production of natural products. Nat Biotechnol. 2015; 33: 377–383. https://doi.org/10.1038/nbt.3095 PMID: 25558867

29. Chen C-Y, Nace GW, Irwin PL. A 6×6 drop plate method for simultaneous colony counting and MPN enumeration of Campylobacter jejuni, Listeria monocytogenes, and Escherichia coli. J Microbiol Methods. 2003; 55: 475–479. https://doi.org/10.1016/S0167-7012(03)00194-5 PMID: 14529971

30. Govan JR, Deretic V. Microbial pathogenesis in cystic fibrosis: mucoid Pseudomonas aeruginosa and Burkholderia cepacia. Microbiol Rev. 1996; 60: 539–574. PMID: 8840786

31. Jones AM, Dodd ME, Govan JRW, Barcus V, Doherty CJ, Morris J, et al. Burkholderia cenocepacia and Burkholderia multivorans: influence on survival in cystic fibrosis. Thorax. 2004; 59: 948–951. https://doi.org/10.1136/thx.2003.017210 PMID: 15516469

32. Eberl L, Tümmler B. Pseudomonas aeruginosa and Burkholderia cepacia in cystic fibrosis: genome evolution, interactions and adaptation. Int J Med Microbiol. 2004; 294: 123–131. https://doi.org/10.1016/j.ijmm.2004.06.022 PMID: 15493822

33. Costello A, Reen FJ, O'Gara F, Callaghan M, McClean S. Inhibition of co-colonizing cystic fibrosis-associated pathogens by Pseudomonas aeruginosa and Burkholderia multivorans. Microbiology. 2014; 160: 1474–1487. https://doi.org/10.1099/mic.0.074203-0 PMID: 24790091

34. Leinweber A, Fredrik Inglis R, Kümmerli R. Cheating fosters species co-existence in well-mixed bacterial communities. ISME J. 2017; 11: 1179–1188. https://doi.org/10.1038/ismej.2016.195 PMID: 28060362

35. Schwarz S, West TE, Boyer F, Chiang W-C, Carl MA, Hood RD, et al. Burkholderia Type VI Secretion Systems Have Distinct Roles in Eukaryotic and Bacterial Cell Interactions. PLOS Pathog. 2010; 6: e1001068. https://doi.org/10.1371/journal.ppat.1001068 PMID: 20865170

36. Hanly TJ, Urello M, Henson MA. Dynamic flux balance modeling of S. cerevisiae and E. coli co-cultures for efficient consumption of glucose/xylose mixtures. Appl Microbiol Biotechnol. 2012; 93: 2529–2541. https://doi.org/10.1007/s00253-011-3628-1 PMID: 22005741

37. Salimi F, Mahadevan R. Characterizing metabolic interactions in a clostridial co-culture for consolidated bioprocessing. BMC Biotechnol. 2013; 13: 95. https://doi.org/10.1186/1472-6750-13-95 PMID: 24188120

38. Junicke H, Abbas B, Oentoro J, van Loosdrecht M, Kleerebezem R. Absolute Quantification of Individual Biomass Concentrations in a Methanogenic Coculture. AMB Express. 2014; 4: 35. https://doi.org/10.1186/s13568-014-0035-x PMID: 24949269

39. Jensen PA, Dougherty BV, Moutinho TJ, Papin JA. Miniaturized Plate Readers for Low-Cost, High-Throughput Phenotypic Screening. J Lab Autom. 2015; 20: 51–55. https://doi.org/10.1177/2211068214555414 PMID: 25366331

40. Liao BQ, Bagley DM, Kraemer HE, Leppard GG, Liss SN. A Review of Biofouling and its Control in Membrane Separation Bioreactors. Water Environ Res. 2004; 76: 425–436. https://doi.org/10.2175/106143004X151527 PMID: 15523788

41. Schalk IJ, Guillon L. Pyoverdine biosynthesis and secretion in Pseudomonas aeruginosa: implications for metal homeostasis. Environ Microbiol. 2013; 15: 1661–1673. https://doi.org/10.1111/1462-2920.12013 PMID: 23126435